Received: 12 June 2019 | Revised: 27 December 2019 | Accepted: 2 January 2020

DOI: 10.1111/jzs.12373

ORIGINAL ARTICLE

JOURNAL OF ZOOLOGICAL SYSTEMATICS AND EVOLUTIONARY RESEARCH

WILEY

Phylogeny of African fruit bats (Chiroptera, Pteropodidae) based on complete mitochondrial genomes

Alexandre Hassanin[1] | Céline Bonillo[2] | Didier Tshikung[3] | Célestin Pongombo Shongo[3] | Xavier Pourrut[4] | Blaise Kadjo[5] | Emmanuel Nakouné[6] | Vuong Tan Tu[7] | Vincent Prié[1] | Steven M. Goodman[8]

[1]Institut Systématique Evolution Biodiversité (ISYEB), Sorbonne Université, MNHN, CNRS, EPHE, Paris, France

[2]Muséum National d'Histoire Naturelle, UMS 2700 2AD, Paris, France

[3]Faculté de Médecine Vétérinaire, Université de Lubumbashi, Lubumbashi, Democratic Republic of the Congo

[4]Institut de Recherche pour le Développement, UR 224, MIVEGEC, Marseille, France

[5]UFR Biosciences, Université Félix Houphouet-Boigny, Abidjan, Côte d'Ivoire

[6]Institut Pasteur de Bangui, Bangui, Central African Republic

[7]Institute of Ecology and Biological Resources, Vietnam Academy of Science and Technology, Hanoi, Vietnam

[8]Field Museum of Natural History, Chicago, IL, USA

Correspondence
Alexandre Hassanin, Institut Systématique Evolution Biodiversité (ISYEB), Sorbonne Université, MNHN, CNRS, EPHE; 57 rue Cuvier, CP 51, 75005 Paris, France.
Email: alexandre.hassanin@mnhn.fr

Abstract

Members of the family Pteropodidae, also known as Old World fruit bats, are represented in Africa by 14 genera and 44 species. Here, we sequenced 67 complete mitochondrial genomes from African and Asian pteropodids to better understand the evolutionary history of the subfamily Rousettinae, which includes most of the African species. An increased frequency of guanine to adenine transitions is detected in the mtDNA genomes of *Macroglossus sobrinus* and all species of *Casinycteris* and *Scotonycteris*. Our phylogenetic and molecular dating analyses based on 126 taxa and 15,448 characters indicate a low signal for deep relationships within the family, suggesting a rapid diversification during the Late Oligocene period of "warming." Within the subfamily Rousettinae, most nodes are highly supported by our different analyses (all nucleotide sites, SuperTRI analyses of a sliding window, transversions only, coding genes only, and amino acid sequences). The results indicate the existence of four tribes: Rousettini—distributed from Africa through Mediterranean region and South Asia to South-East Asia; Eonycterini—found in Asia; and Epomophorini and Scotonycterini—restricted to sub-Saharan Africa. Although most interspecies relationships are highly supported, three parts of the Rousettinae mitochondrial tree are still unresolved, suggesting rapid diversification: (a) among the three subtribes Epomophorina (*Epomophorus* sensu lato, i.e., including *Micropteropus*, *Epomops*, *Hypsignathus*, *Nanonycteris*), Plerotina (*Plerotes*), and Myonycterina (*Myonycteris*, *Megaloglossus*) in the Late Miocene; (b) among *Epomops*, *Hypsignathus*, and other species of Epomophorina at the Pliocene–Pleistocene boundary; and (c) among *Myonycteris* species in the Early Pleistocene. Within the Epomophorini, *Stenonycteris lanosus* emerged first, suggesting that lingual echolocation may have appeared in the common ancestor of Epomophorini and Rousettini. Our analyses suggest that multiple events of mtDNA introgression occurred within the *Epomophorus* species complex during the Pleistocene.

Contributing authors: Céline Bonillo (bonillo@mnhn.fr), Didier Tshikung (didiertshikung@yahoo.fr), Célestin Pongombo Shongo (pongoshon@gmail.com), Xavier Pourrut (xavier.pourrut@ird.fr), Blaise Kadjo (blaisekadjo1@hotmail.com), Emmanuel Nakouné (enakouney@gmail.com), Vuong Tan Tu (tuvuongtan@gmail.com), Vincent Prié (prie.vincent@gmail.com), Steven M. Goodman (sgoodman@fieldmuseum.org)

KEYWORDS
lingual echolocation, mitochondrial base composition, mitochondrial introgression, Plio-Pleistocene, Rousettinae, sub-Saharan Africa

1 | INTRODUCTION

Fruit bats of the family Pteropodidae Gray, 1821 (Mammalia, Chiroptera) are found in all tropical and subtropical regions of the Old World. The classification provided by the African Chiropteran Report (ACR, 2018) recognizes 44 extant African species placed in 14 genera and three subfamilies: Pteropodinae Gray, 1821, Eidolinae Almeida, Giannini, & Simmons, 2016, and Rousettinae Andersen, 1912. The subfamily Pteropodinae is represented by eight species of the genus *Pteropus*, unknown from continental Africa and regionally occurring on offshore islands or isolated on Indian Ocean islands. The subfamily Eidolinae contains only two species in the genus *Eidolon*: *E. helvum*—widely distributed on the continent and offshore islands, and *E. dupreanum*—endemic to Madagascar. According to the ACR (2018), the 12 other Afro-Malagasy genera belong to the subfamily Rousettinae: *Casinycteris* (three species), *Epomophorus* (10 species), *Epomops* (two species), *Hypsignathus monstrosus*, *Megaloglossus* (two species), *Micropteropus* (two species), *Myonycteris* (five species), *Nanonycteris veldkampii*, *Plerotes anchietae*, *Rousettus* (three species), *Scotonycteris* (three species), and *Stenonycteris lanosus*.

Previous molecular studies on the phylogeny of African fruit bats were based on DNA sequences from three mitochondrial genes, corresponding to the protein-coding *cytochrome b* gene and the two genes encoding 12S and 16S ribosomal RNAs (e.g., Almeida et al., 2016; Giannini & Simmons, 2003; Hassanin et al., 2016; Juste et al., 1999; Nesi et al., 2013), and from five nuclear protein-coding genes, corresponding to *C-MOS*, *RAG1*, *RAG2*, *VWF*, *and BRCA1* (Almeida, Giannini, DeSalle, & Simmons, 2011; Almeida et al., 2016; Giannini & Simmons, 2003). Several nuclear introns were also sequenced from species of Myonycterini (seven introns in Nesi et al., 2013) and Scotonycterini (12 introns in Hassanin et al., 2015). Phylogeographic results have led to several taxonomic changes: three new species were described, that is, *Casinycteris campomaanensis*, *Megaloglossus azagnyi*, and *Scotonycteris bergmansi*; and two taxa formerly considered to be subspecies are now treated as full species, that is, *Myonycteris leptodon* and *Scotonycteris occidentalis* (Hassanin, 2014; Hassanin et al., 2015; Nesi et al., 2013).

Previous molecular studies have revealed the existence of a large African clade, including all species except those in the genera *Casinycteris*, *Eidolon*, *Pteropus*, *Rousettus*, and *Scotonycteris* (Almeida et al., 2016; Hassanin et al., 2016; Juste et al., 1999). Within this group, certain relationships remain unresolved, such as the positions of *P. anchietae* and *S. lanosus*. Previous estimations of divergence times were based on *cytochrome b* alignments and the use of either a mean rate of approximately 0.02 substitutions per site per million years (Almeida et al., 2016; Hassanin et al., 2015; Nesi et al., 2013) or a single molecular calibration point (extracted from the study of Meredith et al., 2011) at 16.5 ± 1.5 Mya for the common ancestor of Pteropodidae (Hassanin et al., 2016).

Here, we sequenced the complete mitochondrial genome for 67 individual fruit bats, representing most pteropodid species currently recognized in Africa, and performed comparisons with available mtDNA genomes for Pteropodidae (seven mtDNA genomes) and the nine other bat families (49 mtDNA genomes; Emballonuridae, Hipposideridae, Molossidae, Mormoopidae, Mystacinidae, Noctilionidae, Phyllostomidae, Rhinolophidae, and Vespertilionidae). Our main purposes were to examine phylogenetic relationships among taxa of Rousettinae, and to estimate divergence times within Pteropodidae in order to better understand when fruit bats arrived to the Africa continent, and how they have subsequently diversified.

2 | MATERIALS AND METHODS

2.1 | DNA extraction, amplification, and sequencing

Total DNA was extracted from cells, muscle, patagium, or bone samples using DNeasy Blood and Tissue Kit (Qiagen). Details on the 67 samples extracted for this study are indicated in Appendix 1, which also includes definitions of museum acronyms. The mitochondrial genomes were sequenced using one of the three following approaches: Sanger sequencing of ≈20 overlapping PCR products (length between 700 and 2,000 nt); next-generation sequencing (NGS) of five overlapping long PCR products of around 4–5 kb; and shotgun Illumina sequencing.

In the first approach, PCR amplifications were carried out as detailed in Hassanin et al. (2012) using the primers listed in Table S1. The amplicons were then sequenced in both directions by Eurofins MWG Operon. Genomes were assembled with electropherograms of overlapping amplicons using Sequencher 5.1 (Gene Codes Corporation).

In the second approach, five overlapping PCR products of around 4–5 kb were amplified using the following primer sets: (a) GluCH2 (Hassanin, 2014) and 12SL335-CH (5′-ATC-GTR-TGA-CCG-CGG-TGG-CTG-GCA-CGA-3′); (b) PheU-CH (5′-AGC-RAR-GCA-CTG-AAA-ATG-CYT-AGA-TG-3′) and LMet3-CH (5′-ATT-TTC-GGG-GTA-TGG-GCC-CGA-TAG-CTT-A-3′); (c) IleU (Hassanin et al., 2012) and A8A6L-CH (5′-GGG-GTA-ATR-AAA-GAG-GMR-AAT-ARA-TTT-TCG-3′); (d) SerU-CH (5′-TCG-AAC-CCC-CWN-AWR-TTG-GTT-TCA-AGC-C-3′) and Leu2LM1-CH (5′-GTT-GCA-CCA-ATT-TTT-TGG-YTC-CTA-AG-3′); and (e) Ser2UM1-CH (5′-AGT-ATG-CAA-GAA-CTG-CTA-AYT-CAT-G-3′) and LPro-CH (5′-GTT-TAA-NTA-GAA-YNT-CAG-CTT-TGG-GTG-3′). PCR reactions were

performed in 18 µl with one unit of HotStart LongAmp® Taq DNA polymerase (New England BioLabs), 5X LongAmp Taq Reaction Buffer, 0.4 ng/µl Bovine Serum Albumin, 3.5% DMSO, 300 nM of each primer, and 300 µM of dNTPs. After an initial denaturation of 30 s at 94°C, the DNA was amplified through 45 cycles of 20 s at 94°C, 30 s at 56–62°C, and 15 min at 65°C, with a terminal elongation for 15 min at 65°C. The amplicons were sequenced at the "Service de Systématique Moléculaire" (MNHN) using the Ion Torrent Personal Genome Machine (Thermo Fisher Scientific) following the method described in Hinsinger et al. (2015).

The third approach was based on Illumina shotgun sequencing. It was used for DNA extracts of lower quality, in particular those obtained from museum specimens (e.g., holotype of *Casinycteris ophiodon*: ZMB 5001). DNA samples were quantified with a Qubit® 2.0 Fluorometer using the Qubit dsDNA HS Assay Kit (Thermo Fisher Scientific). Libraries were prepared using the TruSeq® Nano DNA Library Prep kit (Illumina) after pooling 150 ng of total DNA of 10 species belonging to distant taxonomic groups (i.e., different phyla, classes, orders, or families). Libraries were sequenced at the "Institut du Cerveau et de la Moelle épinière" using a NextSeq® 500 system and the NextSeq 500 High Output Kit v2 (300 cycles; Illumina).

The NGS reads generated with either Ion Torrent or Illumina sequencers were assembled by baiting and iterative mapping approach on Geneious® 10.2.2 (Biomatters Ltd.) using available mitochondrial references, including *cytochrome b*, *cytochrome c oxidase subunit I*, *12S* and *16S rRNA* genes. The 67 new mitochondrial genomes generated for this study were annotated on Geneious and deposited in GenBank under accession numbers MN816299–MN816365.

2.2 | Mitochondrial alignments

The 67 mitochondrial genomes produced in this study were compared with other genomes available in NCBI (see accession numbers in Appendix 1) for Pteropodidae (seven genomes) and other families of Chiroptera, that is, Emballonuridae (one genome), Hipposideridae (one genome), Molossidae (three genomes), Mormoopidae (three genomes), Mystacinidae (one genome), Noctilionidae (one genome), Phyllostomidae (14 genomes), Rhinolophidae (seven genomes), and Vespertilionidae (18 genomes). Three additional outgroups from three different orders of Laurasiatherian mammals were used to root the chiropteran tree: *Antilocapra americana* (Cetartiodactyla), *Canis latrans* (Carnivora), and *Ceratotherium simum* (Perissodactyla).

The 126 mitochondrial genomes were aligned under AliView 1.22 (Larsson, 2014). Ambiguous regions for primary homology were excluded from the alignment either for all taxa or only for the most divergent outgroup taxa. To limit the impact of missing data, we also removed from the alignment all indels (insertions of deletions) detected in only one genome. The final alignment, named *mtDNA*, contains 126 taxa and 15,448 nucleotide sites. Three other datasets were used for the analyses: (a) the *mtDNA-Tv* dataset, which corresponds to the *mtDNA* dataset in which the nucleotide G was replaced by A, and the nucleotide T by C (i.e., only transversions); (b) the *PCG-DNA* dataset (10,791 nt), in which all regions other than protein-coding genes were removed, as well as the *ND6* gene (because it is located on the opposite strand of other protein-coding genes); and (c) the *PCG-AA* dataset (3,597 amino acids), which is the translated version of PCG-DNA. All the four datasets used in this study are available at https://osf.io/4py89/.

2.3 | Analysis of base composition

The alignment of protein-coding genes of 126 mitochondrial genomes (*PCG-DNA* dataset) was used to calculate the frequency of the four bases (A, C, G, and T) at each of the three codon positions. The 12 variables measured were then summarized by a principal component analysis (PCA) using the FactoMineR package (Lê, Josse, & Husson, 2008) in R version 3.5.3 (from http://www.R-project.org/). The strand bias in nucleotide composition was studied at third codon positions of the *PCG-DNA* dataset by calculating the relative frequencies of A and T nucleotides (AT3 skew = [A − T]/[A + T]) and the relative frequencies of C and G nucleotides (CG3 skew = [C − G]/[C + G]) (Arabi, Cruaud, Couloux, & Hassanin, 2010; Hassanin, Léger, & Deutsch, 2005; Lobry, 1995).

2.4 | Phylogenetic analyses

The four datasets (*mtDNA*, *mtDNA-Tv*, *PCG-DNA*, and *PCG-AA*) were analyzed with probabilistic methods for tree reconstruction, using the resources available from the CIPRES Science Gateway (Miller, Pfeiffer, & Schwartz, 2010). The maximum-likelihood analyses were conducted using RAxML version 8.2.10 (Stamatakis, 2014) with 25 rate categories (CAT approximation), 1,000 bootstrap replicates, and the GTR model for *mtDNA*, *mtDNA-Tv*, and the three codon positions of *PCG-DNA*, and the mtMAM model for *PCG-AA*. The Bayesian analyses were done with MrBayes 3.2.6 (Ronquist et al., 2012) and the following models: GTR+I+G for *mtDNA* and the three codon positions of *PCG-DNA*, JC69+I+G for *mtDNA-Tv*, and the mixed model for *PCG-AA*. The posterior probabilities (PP) were calculated using 10,000,000 Metropolis-coupled MCMC generations, tree sampling every 1,000 generations, and a burn-in of 25%.

To examine the phylogenetic signal along the *mtDNA* dataset, we also performed Bayesian analyses (with the same parameters) on 10 half-overlapping sub-datasets (a–j) of the about the same length (i.e., 3,090 or 3,088 nt), corresponding to the following positions: (a) 1–3,090; (b) 1,546–4,635; (c) 3,091–6,180; (d) 4,636–7,725; (e) 6,181–9,270; (f) 7,726–10,815; (g) 9,271–12,360; (h) 10,816–13,905; (i) 12,361–15,448; and (j) 13,906–15,448 + 1–1,545. The use of half-overlapping sub-datasets (sliding window of ≈3,090 nt) implies that all nucleotide sites of the total *mtDNA* alignment are represented twice in these Bayesian analyses. The lists of bipartitions obtained from Bayesian analyses of the 10 sub-datasets were transformed into a weighted binary matrix for supertree construction using SuperTRI v57 (Ropiquet, Li, & Hassanin, 2009). Each binary

character corresponds to a node, which was weighted according to its frequency of occurrence in one of the 10 lists of bipartitions. In this manner, the SuperTRI method takes into account both principal and secondary signals, because all phylogenetic hypotheses found during the 10 Bayesian analyses were used for the calculation of the following two reliability indices for each node of interest: (a) the supertree bootstrap percentages (SBP) were obtained from PAUP 4* version 4b10 (Swofford, 2003) after 1,000 bootstrap replicates of the MRP (Matrix Representation with Parsimony) matrix of 1,903 binary characters (reconstructed under SuperTRI v57); and (b) the mean PP percentages (MPP) were directly calculated on SuperTRI v57. The SBP and MPP values were reported on the ML tree found with the total alignment of 15,448 nt (Figure 1). Here, the SuperTRI analyses were conducted to test for phylogenetic signal along the mtDNA genome. If a robust node in the ML tree (BP ≥ 95) is recovered with high SBP (≥95%) and MPP values (≥0.80), it can be concluded that the signal is present all along the mtDNA genome. If a node in the ML tree is recovered with low MPP values (<0.50), it can be concluded that the signal is weak or confined to a few fragments of the mtDNA genome. If there is a robust topological conflict between ML and SuperTRI results, it can be inferred that at least one of the studied genomes was partially contaminated by a mitochondrial DNA sequence from another species or by a nuclear DNA sequence of mitochondrial origin (Numt). An example was published in Hassanin, Bonillo, Nguyen, & Cruaud (2010) for the mitochondrial genomes of domestic goat.

2.5 | Molecular dating

Divergence times were estimated on the CIPRES Science Gateway (Miller et al., 2010) using both *mtDNA* and *mtDNA-Tv* datasets and the Bayesian approach implemented in BEAST v.2.4.7 (Bouckaert et al., 2014). As no sufficiently accurate calibration point (fossil record or biogeographic event) is available for the family Pteropodidae, divergence times were initially estimated using three molecular calibration points extracted from Meredith et al. (2011) (P1 approach), corresponding to the age of the most recent common ancestors (MRCA) of Chiroptera (66.5 ± 1.3 million years ago [Mya]), Hipposideridae + Rhinolophidae (42.2 ± 3.0 Mya), and *Pteropus* + *Nyctimene* (16.4 ± 1.1 Mya). As an alternative approach, named P2, the third calibration was replaced by the MRCA of Pteropodidae (25.0 ± 2.0 Mya), considering that the diversification of the family may have first occurred during the period of Late Oligocene warming (see section 4.2) and that this epoch fits well with the pairwise divergence time of 25.9 Mya provided by http://timetree.org/ for *Pteropus* and *Nyctimene*. Two datasets were used for estimating divergence times: *mtDNA* and *mtDNA-Tv*. The *mtDNA-Tv* dataset was used to limit the misleading effect of highly homoplastic transitions and the important variations in base composition (see section 3.2). We applied a GTR+I+G model for the *mtDNA* alignment (with a proportion of invariants of 0.4155) and JC+I+G for the *mtDNA-Tv* alignment (with a proportion of invariants of 0.6539) and a relaxed-clock model with uncorrelated lognormal distribution for substitution rates. Node ages were estimated using a calibrated Yule speciation prior and 10^8 generations, with tree sampling every 1,000 generations, and a burn-in of 25%. MCMC mixing efficiency and convergence were assessed using the ESS values in Tracer v.1.6. The chronogram was reconstructed with TreeAnnotator, which is included in the BEAST package (Bouckaert et al., 2014).

3 | RESULTS

3.1 | Mitochondrial genome of Pteropodidae

The mitochondrial genome was sequenced, assembled, and characterized for 67 fruit bats. The new mitogenomes, which are circular double-stranded DNA sequence of 16,415–16,897 bp in size, show the same organization as in other mammals, with 13 protein-coding genes, 22 transfer RNAs (tRNA), two ribosomal RNAs (rRNAs), and a non-coding region corresponding to the control region (D-loop). Among these genes, only *ND6* and eight tRNAs are encoded by the light strand, whereas the others are encoded by the heavy strand.

The control region of the mtDNA genome of Pteropodidae contains a RS3 repetitive sequence located between CSB1 and CSB2 (Hoelzel, Lopez, Dover, & O'Brien, 1994), which is characterized by several tandem repeats (*n*) of similar motifs: (a) "CATACACGTACG" (*n* = 17–35) in *Dobsonia*, *Eidolon*, *Epomophorus crypturus*, *E. gambianus*, *E. labiatus*, *E. minimus*, *E. minor*, *Epomophorus* sp1, *Epomops buettikoferi*, *Micropteropus pusillus*, *Myonycteris relicta*, *Nanonycteris*, *Plerotes*, *Rousettus aegyptiacus*, *R. leschenaultii*, *R. madagascariensis*, *R. obliviosus*, and *Stenonycteris*; (b) "CATACGCATACG" (*n* = 4–31) in *Cynopterus*, *Epomophorus wahlbergi* (MNHN ZM 2011-800), *Pteropus*, Scotonycterini, and *Sphaerias*; (c) "CATACACGCACG" (*n* = 5–25) in *Epomophorus dobsonii*, *Epomophorus* sp2, *E. wahlbergi* (FMNH 187408

FIGURE 1 Phylogeny of Pteropodidae based on complete mitochondrial genomes. The tree was reconstructed under RAxML using the *mtDNA* dataset (126 taxa and 15,448 nt). For convenience, relationships involving families other than Pteropodidae are not shown here, but the complete phylogenetic tree is available in Figure S1. Taxa found in Africa are written in blue, whereas cave-roosting species are highlighted with a cave icon. For nodes supported by bootstrap percentages (BP) >75, the values correspond from left to right to BP, posterior probabilities (PP), and supertree bootstrap percentages (SBP; an asterisk is used when BP ≥95, PP ≥0.95 and SBP ≥95) followed by the mean PP percentages value calculated on SuperTRI based on the separate analyses of 10 overlapping partitions of the *mtDNA* alignment (see main text for details). No other information was provided for nodes supported by BP <75. Colored circles indicate that the node was also supported by three other ML analyses based on the *mtDNA-Tv* dataset (transversions only), *PCG-DNA* dataset (three codon positions of protein genes), and *PCG-AA* dataset (amino acid alignment; green), only two of them (yellow), or one of them (orange). All branches highlighted in red are interpreted as not reliable

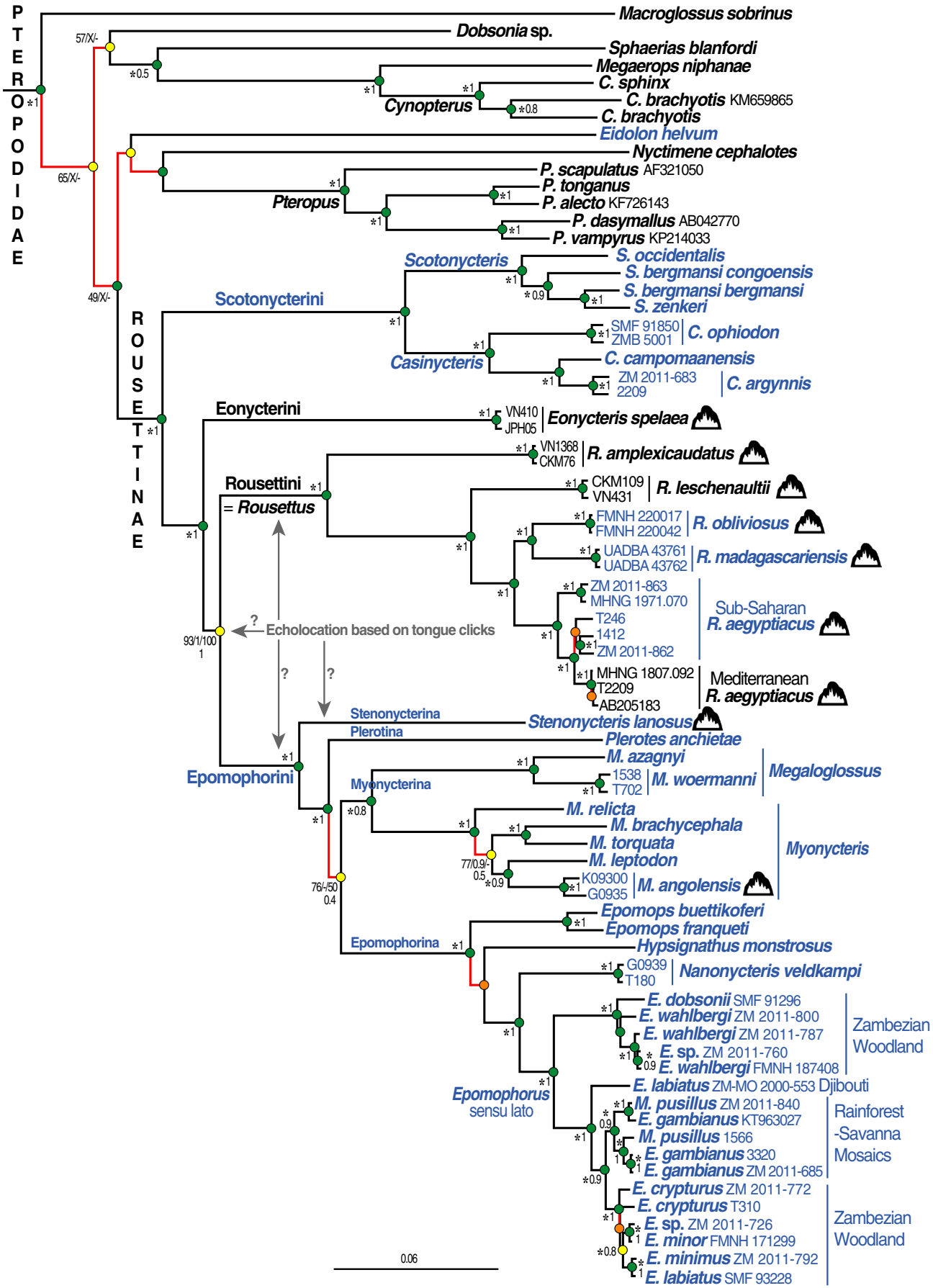
PTEROPODIDAE
ROUSETTINAE
Macroglossus sobrinus
Dobsonia sp.
Sphaerias blanfordi
Megaerops niphanae
C. sphinx
Cynopterus
C. brachyotis KM659865
C. brachyotis
Eidolon helvum
Nyctimene cephalotes
P. scapulatus AF321050
P. tonganus
Pteropus
P. alecto KF726143
P. dasymallus AB042770
P. vampyrus KP214033
Scotonycteris
S. occidentalis
S. bergmansi congoensis
S. bergmansi bergmansi
S. zenkeri
Scotonycterini
SMF 91850
ZMB 5001
C. ophiodon
Casinycteris
C. campomaanensis
ZM 2011-683
2209
C. argynnis
Eonycterini
VN410
JPH05
Eonycteris spelaea
VN1368
CKM76
R. amplexicaudatus
Rousettini
= Rousettus
CKM109
VN431
R. leschenaultii
FMNH 220017
FMNH 220042
R. obliviosus
UADBA 43761
UADBA 43762
R. madagascariensis
ZM 2011-863
MHNG 1971.070
T246
1412
ZM 2011-862
Sub-Saharan
R. aegyptiacus
MHNG 1807.092
T2209
AB205183
Mediterranean
R. aegyptiacus
Echolocation based on tongue clicks
Stenonycterina
Stenonycteris lanosus
Plerotina
Plerotes anchietae
Epomophorini
M. azagnyi
1538
T702
M. woermanni
Megaloglossus
Myonycterina
M. relicta
M. brachycephala
M. torquata
M. leptodon
Myonycteris
K09300
G0935
M. angolensis
Epomops buettikoferi
Epomops franqueti
Epomophorina
Hypsignathus monstrosus
G0939
T180
Nanonycteris veldkampi
E. dobsonii SMF 91296
E. wahlbergi ZM 2011-800
E. wahlbergi ZM 2011-787
E. sp. ZM 2011-760
E. wahlbergi FMNH 187408
Zambezian Woodland
Epomophorus sensu lato
E. labiatus ZM-MO 2000-553 Djibouti
M. pusillus ZM 2011-840
E. gambianus KT963027
M. pusillus 1566
E. gambianus 3320
E. gambianus ZM 2011-685
Rainforest -Savanna Mosaics
E. crypturus ZM 2011-772
E. crypturus T310
E. sp. ZM 2011-726
E. minor FMNH 171299
E. minimus ZM 2011-792
E. labiatus SMF 93228
Zambezian Woodland
0.06

and MNHN ZM 2011-787), *Macroglossus*, *Myonycteris angolensis*, *My. leptodon*, *Nyctimene*, *Rousettus amplexicaudatus*, and specimen 1,538 of *Megaloglossus woermanni* (after several motif e, see below); (d) "CGTACACGTACA" (*n* = 7–24) in *Epomops franqueti*, *Myonycteris brachycephala*, and *Sphaerias* (after several motifs b, see above); (e) "CGTACACGCACG" (*n* = 6–25) in *Hypsignathus*, *M. woermanni*, and *Myonycteris torquata*; (f) "TATACACGCACG" (*n* = 6–8) in *M. azagnyi* and *Nyctimene* (after several motifs c, see above); (g) "CATATACGCACG" (*n* = 4) in *E. wahlbergi* (MNHN ZM 2011-787; after several motifs c, see above); (8) "CGTACACGCA" (*n* = 8–26) in *Eonycteris*; and (9) "CATACGCATGCACACG" (*n* = 6) in *Megaerops*.

3.2 | Evidence for variation in base composition

The base composition (frequency of the nucleotides A, C, G, and T) was analyzed at the three codon positions of the *PCG-DNA* dataset (Table S2). The 12 variables measured for 126 taxa were summarized by a PCA based on the first two principal components (PC), which contribute 43.08% and 26.90% of the total variance, respectively (individuals graph of Figure 2). The variable graph shows that the variance can be explained by differences in base composition at the three codon positions. All pteropodids are found near the middle of the graph, except Scotonycterini and *Macroglossus*, for which the mtDNA genome contains a higher percentage of adenine (33.59% < A < 34.49% vs. "mean in other Pteropodidae" [MoP] = 30.90%). This trend is observed at each of the three codon positions, and is more marked at first and third positions (Table S2): A1 > 33.05% versus MoP = 31.48%; A2 > 19.65% versus MoP = 19.51%; A3 > 48.01% versus MoP = 41.70%. At first and third codon positions, both Scotonycterini and *Macroglossus* have lower percentages of guanine than other pteropodids (Table S2): G1 < 19.49% versus MoP = 20.74%; G3 < 3.98% versus MoP = 6.14%. A similar trend, although less marked, is also observed at third codon positions of the genome of *Dobsonia* (A3 = 47.90%; G3 = 3.95%) and *Sphaerias* (A3 = 45.76%; G3 = 4.06%; Table S2).

The mtDNA genomes of Vespertilionidae are characterized by the highest percentages of thymine (e.g., *Lasiurus*: 33.29%) and the lowest percentages of cytosine (e.g., *Lasiurus*: 22.52%; Table S2). The mtDNA genomes of Phyllostomidae show a marked heterogeneity in base composition (Figure 2): *Desmodus*, *Vampyrum*, *Diaemus*, and *Chrotopterus* have a C-rich genome (>32.66%); *Artibeus* and *Hsunycteris* have a T-rich genome (>31.71%); and *Tonatia* and *Diphylla* have an A-rich genome (>31.58%).

3.3 | Phylogeny of Rousettinae

The ML tree of Figure 1 was reconstructed from the *mtDNA* alignment (the Bayesian tree is provided in Figure S2). The results show that 60 nodes were highly supported by ML and Bayesian analyses, with BP ≥95 and PP ≥0.95 (nodes with an asterisk, also characterized by SBP ≥95). Fifty-nine of these nodes were characterized by MPP ≥0.8 in the SuperTRI analyses, indicating that the phylogenetic signal is robust in all parts of the *mtDNA* alignment, and 59 of these nodes were recovered in all analyses based on the three other datasets (*mtDNA-Tv*, *PCG-DNA*, and *PCG-AA*; nodes highlighted by green circles in Figure 1). Among the highly supported nodes are all the following taxa represented by at least two members in our analyses: family Pteropodidae; subfamily Rousettinae, tribes Epomophorini, Rousettini, and Scotonycterini; genera *Casinycteris*, *Cynopterus*, *Epomops*, *Epomophorus* sensu lato (i.e., including *M. pusillus*), *Megaloglossus*, *Myonycteris*, *Pteropus*, *Rousettus*, and *Scotonycteris*. All species are also found to be monophyletic, except (a) *S. bergmansi*, which was paraphyletic due to the inclusive position of *Scotonycteris zenkeri*; and (b) several species of the *Epomophorus* sensu lato complex, such as *M. pusillus*, *E. gambianus*, and *E. labiatus*, which are found to be polyphyletic.

Only a few nodes are poorly supported by our analyses (indicated in red in Figure 1): all deep relationships within Pteropodidae; interrelationships among the subtribes Epomophorina, Myonycterina, and Plerotina; interrelationships among *Epomops*, *Hypsignathus*, and the clade uniting *Epomophorus* sensu lato and *Nanonycteris*; the early divergence of *My. relicta* from other species of *Myonycteris*; and some intraspecific relationships in *R. aegyptiacus*.

3.4 | Molecular estimates of divergence times

Our molecular estimates of divergence times show that the ages inferred from the *mtDNA* dataset are older than those obtained from the *mtDNA-Tv* dataset (Table S3). The same trend was found when using P1 or P2 calibration approaches. These results can be related to the fact that transitions are more rapidly saturated than transversions and that saturation severely compresses basal branch lengths, which results in overestimated divergence dates for recent nodes. In agreement with that, the deepest nodes of the chronograms estimated with the *mtDNA* dataset have smaller credible intervals (i.e., highest posterior density intervals at 95%) than those estimated with the *mtDNA-Tv* dataset. On the contrary, the most recent nodes (i.e., relationships within tribes, <14 Mya) estimated with the *mtDNA* dataset have larger credible intervals than those estimated with the *mtDNA-Tv* dataset (Table S3). Therefore, we conclude that the ages estimated from the *mtDNA-Tv* dataset are more accurate and reliable than those estimated from the *mtDNA* dataset. The divergence times estimated with the *mtDNA-Tv* dataset and using either P1 or P2 calibration approaches are notably similar for most nodes, but the differences are more important for the deepest nodes of the pteropodid tree (Table 1).

4 | DISCUSSION

4.1 | Higher rates of G-to-A transitions in *Macroglossus* and Scotonycterini

Since cytosine and adenine deaminations are known to occur more frequently on single-stranded DNA than double-stranded DNA, they accumulate more rapidly on the heavy strand during

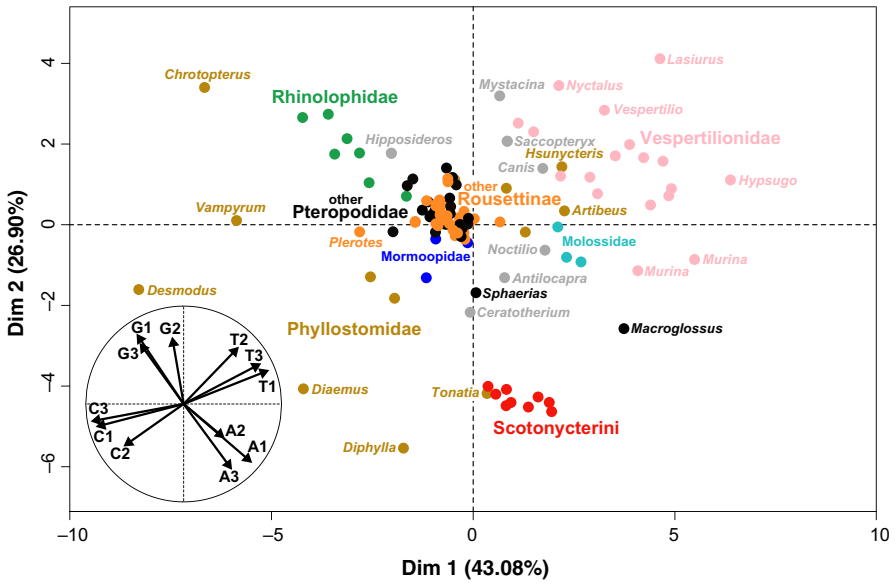

FIGURE 2 Principal component analysis of base composition. The *PCG-DNA* dataset was used to calculate the frequency of the four bases (A, C, G, and T) at each of the three codon positions, and the 12 variables measured were then summarized by a principal component analysis (PCA). The main graph represents the individual factor map, in which animals are colored according to their taxonomic assignation. Members of the family Pteropodidae are indicated by three colors: red for Scotonycterini, orange for other Rousettinae, and black for other Pteropodidae. Other chiropteran families represented by several taxa are also indicated by colors: Molossidae in light blue, Mormoopidae in navy blue, Phyllostomidae in light brown, Rhinolophidae in green, and Vespertilionidae in light pink. Isolated genera are shown in gray. The small circular graph at the bottom left represents the variables factor maps

replication and transcription. As a consequence, the heavy strand of the mitochondrial genome of mammals is A + C poor; the light strand is A + C rich and this strand bias in nucleotide composition can be easily detected at third codon positions, where all transitions are synonymous (Hassanin et al., 2005; Reyes, Gissi, Pesole, & Saccone, 1998). The light strand of the mtDNA genomes of Pteropodidae contains 40.0%–50.6% of adenine, 26.5%–38.4% of cytosine, 14.5%–20.6% of thymine, and 2.3%–7.8% of guanine (Table S2). Our analyses revealed that the mitochondrial genomes of *Macroglossus* and Scotonycterini have different base compositions than those of other Pteropodidae (Figure 2), with a higher frequency of adenine associated with a lower frequency of guanine at the three codon positions. These results indicate that G-to-A substitutions occurred more frequently on the light strand of the mtDNA genome of *Macroglossus* and Scotonycterini. Such changes in mutational pattern can be related to an increased rate of cytosine deamination on the heavy strand of mtDNA, leading to C → T transitions on the heavy strand and therefore G → A transitions on the light strand (Hassanin et al., 2005; Hassanin, Ropiquet, Couloux, & Cruaud, 2009). Three non-exclusive hypotheses can account for higher levels of cytosine deamination on the heavy strand of the mitochondrial genome of *Macroglossus* and Scotonycterini: more severe oxidative stress (due to a higher production of reactive oxygen species in mitochondria), higher metabolic rates (Hassanin et al., 2009), and more rapid cell division. Collecting physiological data on fruit bats is needed to evaluate the respective contribution of these three potential mechanisms.

4.2 | Rapid diversification of Pteropodidae during the Oligocene

Most nodes of the tree presented in Figure 1 can be considered robust, as they were monophyletic in all analyses of the four datasets (*mtDNA*, *mtDNA-Tv*, *PCG-DNA*, and *PCG-AA*) and also supported by high SuperTRI values. Among them, all the following supra-specific taxa are found monophyletic with the four datasets and supported by BP and SBP >95, PP >0.95, and MPP >0.8 with the *mtDNA* dataset: Pteropodidae, Rousettinae, Rousettini (=*Rousettus*), Eonycterini, Epomophorini, Scotonycterini, Epomophorina, Myonycterina, *Casinycteris*, *Cynopterus*, *Epomophorus* sensu lato (see details below), *Epomops*, *Megaloglossus*, *Myonycteris*, *Pteropus*, and *Scotonycteris*. By contrast, deep nodes within Pteropodidae were interpreted as unresolved, because relationships among Rousettinae, *Cynopterus* + *Megaerops* + *Sphaerias*, *Dobsonia*, *Eidolon*, *Macroglossus*, *Nyctimene* + *Pteropus* were conflicting between phylogenetic trees based on the four datasets (Figure S1) and not supported by SuperTRI analyses of the *mtDNA* dataset (SBP < 50; MPP ≤ 0.3). In particular, the root of the pteropodid tree was found to be unstable between the different trees obtained from RAxML analyses of the four datasets: the first taxon to diverge was *Macroglossus* in both *mtDNA* and *mtDNA-Tv* trees (BP = 65 and 52, respectively), *Dobsonia* in the *PCG-AA* tree (BP = 42), and the group uniting *Dobsonia* with *Cynopterus*, *Megaerops*, and *Sphaerias* (BP = 68) in the *PCG-DNA* tree (BP = 40). Such a lack of resolution for the deepest relationships within Pteropodidae was also found in previous molecular studies, based on either many nuclear

TABLE 1 Mean node ages (in bold and 95% highest posterior density intervals between brackets) in million years ago (Mya) estimated with the *mtDNA-Tv* dataset and two different calibrations (P1: MRCA of *Pteropus* + *Nyctimene*; P2: MRCA of Pteropodidae)

	P1 16.4 ± 1.1 Mya	P2 25.0 ± 2.0 Mya
Pteropodidae + Hipposideridae + Rhinolophidae	**59.0** (63.7–54.0)	**58.4** (63.4–52.6)
Family Pteropodidae	**31.2** (36.0–26.3)	**27.0** (29.1–25.0)
Basal diversification of fruit bats	**31.2–23.1** (36.0–19.9)	**27.0–17.9** (29.1–14.2)
Subfamily Rousettinae	**19.3** (22.6–16.2)	**18.4** (21.0–15.8)
Rousettini + Eonycterini + Epomophorini	**15.7** (18.6–12.8)	**15.0** (17.5–12.3)
Rousettini + Epomophorini	**13.6** (16.3–10.8)	**13.0** (15.3–10.5)
Tribe Scotonycterini	**7.7** (10.0–5.4)	**7.3** (9.7–5.0)
Genus *Scotonycteris*	**2.6** (3.6–1.7)	**2.5** (3.5–1.7)
S. zenkeri + *S. bergmansi*	**2.0** (2.8–1.2)	**1.9** (2.7–1.2)
S. zenkeri + *S. bergmansi bergmansi*	**0.9** (1.4–0.4)	**0.8** (1.3–0.4)
Genus *Casinycteris*	**3.2** (4.5–2.0)	**3.1** (4.3–1.9)
C. argynnis + *C. campomaanensis*	**1.2** (1.8–0.7)	**1.2** (1.7–0.7)
Tribe Rousettini = Genus *Rousettus*	**7.2** (9.8–4.9)	**6.7** (8.9–4.5)
All *Rousettus* but *R. amplexicaudatus*	**2.1** (3.0–1.4)	**2.1** (2.8–1.3)
R. aegyptiacus + *R. madagascariensis* + *R. obliviosus*	**1.2** (1.7–0.8)	**1.2** (1.6–0.8)
R. madagascariensis + *R. obliviosus*	**0.9** (1.3–0.5)	**0.9** (1.3–0.5)
R. aegyptiacus	**0.5** (0.7–0.3)	**0.5** (0.7–0.3)
Tribe Epomophorini	**8.5** (10.5–6.6)	**8.1** (9.8–6.4)
Subtribes Epomophorina + Myonycterina + Plerotina	**6.6** (8.1–5.1)	**6.3** (7.4–4.7)
Subtribe Epomophorina	**2.8** (3.6–2.1)	**2.7** (3.5–2.0)
Genus *Epomops*	**0.4** (0.7–0.2)	**0.4** (0.7–0.2)
Epomophorus + *Nanonycteris*	**1.9** (2.6–1.3)	**1.9** (2.5–1.3)
Genus *Epomophorus* sensu lato	**1.3** (1.8–0.8)	**1.2** (1.7–0.8)
E. dobsonii + *E. wahlbergi*	**0.5** (0.7–0.3)	**0.5** (0.7–0.3)
E. crypturus + *E. gambianus* + *E. labiatus* + *Micropteropus pusillus*	**0.5** (0.7–0.3)	**0.5** (0.6–0.3)
E. gambianus + *M. pusillus* (species of rainforest–savanna mosaics)	**0.3** (0.6–0.2)	**0.3** (0.6–0.2)
E. crypturus + other small species of the Zambezian woodland	**0.2** (0.4–0.1)	**0.2** (0.4–0.1)
Subtribe Myonycterina	**5.0** (6.5–3.7)	**4.8** (6.2–3.5)
Genus *Myonycteris*	**2.0** (2.6–1.4)	**1.9** (2.5–1.3)
All *Myonycteris* but *My. relicta*	**1.8** (2.4–1.2)	**1.7** (2.2–1.2)
My. angolensis + *My. leptodon*	**1.3** (1.9–0.8)	**1.3** (1.8–0.8)
Genus *Megaloglossus*	**1.0** (1.6–0.5)	**1.0** (1.6–0.5)

loci (17 nuclear genes, 13.7 kb) sequenced for only four genera of Pteropodidae (*Cynopterus*, *Nyctimene*, *Pteropus*, and *Rousettus*; Teeling et al., 2005) or six molecular markers sequenced for a larger taxonomic dataset (36 genera of Pteropodidae; dataset 1 analyzed in Almeida et al., 2011). As in the nuclear study of Almeida et al. (2011), we found high support for nodes that are more ancient (and also more recent) than the diversification of the crown group of Pteropodidae. The hypothesis involving a rapid diversification of the family is therefore supported by both mitochondrial and nuclear datasets. However, there is no consensus for the age of this radiation: 20–29 Mya in Teeling et al. (2005); 22–41 Mya in Shi & Rabosky (2015), 19.4–19.5 Mya in Almeida et al. (2016) and Hassanin et al. (2016), but with large 95% credible intervals; and 25.9 Mya in Amador, Moyers Arévalo, Almeida, Catalano, & Giannini (2018). The molecular dating of pteropodid diversification remains problematic because no reliable fossils older than the Plio-Pleistocene can be used to calibrate molecular dating analyses. As discussed in Gunnell & Simmons (2005), the oldest fossils assigned to Pteropodidae were found in the Late Eocene/Early Oligocene of Thailand, Late Oligocene/Middle Miocene of France, Early Miocene of Africa, and Late Miocene of China. However, these specimens are too fragmentary to be definitively referred to any extant taxon. Hence, based on current information, fossil calibration cannot be used for estimating divergence times among Pteropodidae. As a consequence, molecular dating studies have been based on either a mean rate of substitutions for *Cytb* gene

sequences (Almeida et al., 2011, 2016; Hassanin et al., 2015; Nesi et al., 2013) or a selection of molecular calibration points (Hassanin et al., 2016; present study). Since these methods can be misleading for estimating divergence times, we consider that the crown diversification of Pteropodidae is still unresolved.

As detailed above, the MRCA of Pteropodidae has been dated between 29.0 and 19.4 Mya in previous studies. During this time span, the Late Oligocene, around 25 ± 2 Mya, is known to have been a period of warming (Zachos, Pagani, Sloan, Thomas, & Billups, 2001; Zhang, Pagani, Liu, Bohaty, & Deconto, 2013), which may have favored the expansion of evergreen forests and associated diversification of flowering plants, and, in parallel, fruit consuming bats. Therefore, we applied two different approaches for our molecular dating analyses. The first approach, named P1 in Table 1, was based on three calibration points extracted from the molecular study of Meredith et al. (2011): two points are external to the pteropodid tree; the third point represents the MRCA of *Pteropus* and *Nyctimene* (16.4 ± 1.1 Mya). The second approach, named P2 in Table 1, was based on the two same external points, but the MRCA of Pteropodidae was constrained at 25 ± 2 Mya, assuming a diversification during the Late Oligocene. The ages estimated with these two approaches (P1 and P2 in Table 1) show notable similarities for most nodes, but the differences are more important for deep divergences within the family. Although the MRCA of Pteropodidae was estimated to be older with P1 (31.2 Mya vs. 27.0 Mya with P2), both dating strategies agree with an Oligocene diversification of the main Pteropodidae lineages.

4.3 | Evidence for multiple dispersals from Asia to Africa

As pointed out in Hassanin et al. (2016), three lines of evidence support a South-East Asian origin of Pteropodidae: (a) more than 50% of the total species diversity of the family is found today in this region (IUCN, 2019); (b) Sumatra, Borneo, and Sulawesi contain the highest species density at a given site (>15 species) (Hassanin et al., 2016); and (c) the oldest fossil assigned to this family dates from the Late Eocene/Early Oligocene of Thailand (Ducrocq, Jaeger, & Sige, 1993). In agreement with previous molecular studies (Almeida et al., 2016; Amador et al., 2018; Giannini & Simmons, 2003; Hassanin et al., 2016; Juste et al., 1999), our phylogenetic analyses suggest that the African continent was colonized by at least four Asian lineages (Table 1): between 2.1 and 1.2 Mya for *Rousettus*; between 13.6/13.0 and 8.5/8.1 Mya for Epomophorini; between 19.3/18.4 and 7.7/7.3 Mya for Scotonycterini; and between 27.0/24.5 and 6.9 Mya (date published in Shi et al., 2014 for the divergence between *E. helvum* and *E. dupreanum*) for *Eidolon*.

For *Rousettus*, a simple biogeographic scenario can be proposed on the basis of our analyses, and available geographic and ecological data. First, the geographic range of *R. aegyptiacus* is unique among African fruit bat species, because it covers not only sub-Saharan Africa, but also much of the Middle East, from the eastern part of the Mediterranean region, through the Arabian Peninsula to Iran and western Pakistan (IUCN, 2019). The three species closely related to *R. aegyptiacus* (Figure 1) have peripatric distributions (IUCN, 2019): (a) *R. leschenaultii* is found from eastern Pakistan to Indonesia through the Indian subcontinent, southern China, and mainland South-East Asia; (b) *R. obliviosus* is confined to three of the four islands in the Comoros Archipelago; and (c) its sister species, *R. madagascariensis*, is endemic to Madagascar. As previously found in the molecular studies of Almeida et al. (2016) and Hassanin et al. (2016), the basal position of the other continental Asian species, *R. amplexicaudatus*, suggests a first Pleistocene dispersal event from Asia to Africa through the Middle East between 2.1 and 1.2 Mya, followed by more recent oceanic dispersal events from East Africa to the Comoros (≈300 km) and then Madagascar (≈300 km) between 1.2 and 0.9 Mya. This scenario is supported by the fact that extant *Rousettus* are capable of long-distance dispersal (up to 500 km on the African continent; Happold & Happold, 2013). By comparison with other fruit bats, *Rousettus* spp. are characterized by an exceptional ecological flexibility, as they use lingual echolocation with remarkable precision (Yovel, Geva-Sagiv, & Ulanovsky, 2011), are able to roost in the dark zones of caves, exploit a wide range of food resources (fruits, flowers, pollen, and leaves), and occur across a wide elevational range (lowlands up to 4,000 m) in mesic to dry habitats (Happold & Happold, 2013). As a consequence, *Rousettus* spp. can overcome certain biogeographic barriers that are presumably impassable for other fruit bats. In addition, the more humid conditions that prevailed between 3.5 and 1.2 Mya in the Tuwaiq valley systems of the Arabian Peninsula (Kürschner, 1998) may have provided a dispersal corridor for *Rousettus* from Asia to Africa.

The three other African lineages of fruit bats, that is, *Eidolon*, Epomophorini, and Scotonycterini, have less flexible ecological characteristics than *Rousettus*, implying that their Asian ancestors were able to colonize Africa through the Middle East only when more favorable humid conditions occurred during the Neogene. Based on our divergence time estimates, we suggest that their ancestors entered in Africa during the Miocene. This epoch was a key period for faunal interchanges between Africa and Asia, because the eastern Tethys seaway was closed off by the meeting of the Afro-Arabian and Eurasian tectonic plates (Hamon, Sepulchre, Lefebvre, & Ramstein, 2013; Meulenkamp & Sissingh, 2003). Two Miocene periods appear to be suitable for a forest corridor in the Middle East: the Middle Miocene Climatic Optimum (MMCO) at 16 ± 1 Mya, and the Tortonian stage between 11.6 and 7.2 Mya. The warmer and more humid conditions prevailing during the MMCO (Zachos, Dickens, & Zeebe, 2008) enhanced the expansion of evergreen forests in North Africa, South and Central Europe, Anatolia, and India (Biltekin et al., 2015; Patnaik, 2016; Senut, Pickford, & Ségalen, 2009; Utescher, Mosbrugger, Ivanov, & Dilcher, 2009). Our molecular dating indicates that both *Eidolon* and Scotonycterini ancestors may have migrated from Asia into Africa during the MMCO via an evergreen forest corridor. By contrast, the ancestor of Epomophorini dispersed more recently to Africa. During the Tortonian, the climate of northeastern Africa and Arabian Peninsula

was less arid than today, but the Middle East route was too dry for the growth of megathermic plants, which may have prevented the dispersal of obligate humid forest vertebrates (Kürschner, 1998; Pound et al., 2011). It seems therefore that only two ecological categories of bats were able to colonize Africa during the Late Miocene: cave-roosting species, which may have proceeded by step migration along the riverine forests of the Arabian Peninsula, and robust species that can fly long distances from one forest patch to another one. Several arguments developed in the next paragraph suggest that the ancestor of Epomophorini was indeed a cave-dwelling. The current ecological characteristics of *Eidolon* species, including their great flight endurance (Richter & Cumming, 2008) and resistance to high temperatures (Happold & Happold, 2013) indicate that the ancestor of *Eidolon* was also able to disperse during the Tortonian. By contrast, the hypothesis is less credible for Scotonycterini, as their ancestor was probably highly dependent on humid forests, as are all the six extant species of the tribe (Hassanin et al., 2015). An African dispersal during the MMCO seems therefore a more likely hypothesis for Scotonycterini.

4.4 | Stenonycteris, a key taxon to understand the evolution of lingual echolocation

Boonman, Bumrungsri, & Yovel (2014) have shown that three species of Asian fruit bats can produce click sounds in the dark by wing clapping: *Cynopterus brachyotis*, *Eonycteris spelaea*, and *Macroglossus sobrinus*. Since these taxa represent distinct lineages in the Pteropodidae phylogeny, these authors have suggested that rudimentary echolocation based on wing clicks may concern all fruit bats. Moreover, *R. aegyptiacus* can emit wing clicks in addition to their lingual echolocation. The co-occurrence of the two mechanisms in *R. aegyptiacus* implies that echolocation based on tongue double clicks evolved independently from echolocation based on wing clicks. In addition to *R. aegyptiacus*, lingual echolocation has been described in *R. madagascariensis* (Schoeman & Goodman, 2012) and in Asian *R. amplexicaudatus* (Roberts, 1975) and *R. leschenaultii* (Raghuram, Gopukumar, & Sripathi, 2007). All these data indicate that lingual echolocation was already present in the common ancestor of *Rousettus*. Since all *Rousettus* species are cave-dwelling, this more sophisticated system was probably selected to improve navigation within cave systems.

Kingdon (1974) wrote that *S. lanosus* is "able to fly in utter darkness, uttering a rapid succession of chinks, that seem to me to be quieter and more 'musical' than the clicks of *Rousettus*." This observation suggests that *S. lanosus* can also use lingual echolocation to fly in the complete darkness of caves, where it is known to roost (Kingdon, 1974). In certain classifications, this species is included in the genus *Rousettus* (Happold & Happold, 2013; IUCN, 2019). However, Kingdon (1974) placed the species into its own genus *Stenonycteris* based on distinct morphological traits, such as narrow cheek teeth, tilted skull, ears shape, elongated tibiae, and long hairs. This view was corroborated by the molecular study of Nesi et al. (2013) and all subsequent studies (Almeida et al., 2016; Hassanin et al., 2016; herein). The position of *Stenonycteris* with respect to other Epomophorini (subtribes Epomophorina, Myonycterina, and Plerotina) was previously unstable and poorly supported in different published studies (BP < 50) (Almeida et al., 2016; Hassanin et al., 2016). By contrast, our mitogenomic analyses provide maximal support for an early divergence of *Stenonycteris* (Stenonycterina) within the tribe Epomophorini (BP = 100; PP = 1; MPP = 1).

In agreement with this topology, two scenarios can be proposed for the evolution of lingual echolocation: (a) convergent adaptation in *Rousettus* and *Stenonycteris* due to independent colonization of cave environments; or (b) acquisition of lingual echolocation in the ancestor of Epomophorini + Rousettini followed by a single loss in the ancestor of Epomophorina + Myonycterina + Plerotin a. Ecologically, it is likely that cave-roosting constituted a crucial step for the dispersal of the ancestor of Epomophorini from Asia to Africa, through the Middle East. Although most extant species of Epomophorini have day roosts in trees, two lines of evidence suggest that their ancestor was able to roost in caves. Firstly, two living species of Epomophorini are known to be cave-roosting bats, that is, *S. lanosus*, which occupies a basal phylogenetic position in the tribe, and *My. angolensis*, which has a more inclusive position (Figure 1). Secondly, the closest relatives to Epomophorini are the tribes Eonycterini and Rousettini (Figure 1), in which all species are known to roost in caves (IUCN, 2019).

Cave-roosting has many advantages for bats, as caves provide protection against most predators and a buffer against fluctuations in temperature and adverse weather (Kunz, 1982). In the order Chiroptera, cave-roosting taxa represent <40% of the total species diversity (IUCN, 2019), but their wide geographic distribution shows that they succeeded in colonizing higher latitudes, with colder average annual temperature, as well as the Sahara, the largest and hottest desert in the world. In the Pteropodidae, only 34 species are known to roost in caves, but their distribution covers most of the family's distribution (IUCN, 2019), suggesting a higher capacity for trans-continental dispersal. We consider therefore that the proposed cave-roosting behavior of the ancestor of Epomophorini probably played an important role for its Miocene dispersal from Asia to Africa. In sub-Saharan Africa, associated with the type of surface bedrock, caves are less common than in Eurasia, suggesting higher interspecific competition among cave-dwelling bats from a range of different families for roosting sites. Although lingual echolocation has been conserved in the ancestor of Stenonycterina in East Africa, where caves are relatively common, it can be assumed that the common ancestor of Epom ophorina + Myonycterina + Plerotina had to change its roosting preferences, from caves to trees, which may have been associated with the loss of echolocation capacity. This change of roost type probably explains their successful subsequent diversification in sub-Saharan Africa, with 24 extant species found in most habitat types, including forest, savanna, shrubland, and grassland (ACR, 2018; IUCN, 2019).

4.5 | The *Epomophorus* species complex: a taxonomic imbroglio to be solved

The *Epomophorus* species complex is the least resolved taxonomic group of African Pteropodidae. In Figure 1, this taxon was named "*Epomophorus* sensu lato" to indicate that it contains all species of *Epomophorus* (including *E. dobsonii*, which was formerly treated as a species of *Epomops*) and *M. pusillus* (originally considered as a species of *Epomophorus*, but generally excluded from this genus because of its small body size and a different soft palate; Bergmans, 1989). The close similarity between mitochondrial sequences (*CO1* and *Cytb*) of *E. gambianus* and *M. pusillus* was first mentioned by Nesi, Nakouné, Cruaud, & Hassanin (2011). Thereafter, this pattern was confirmed by Almeida et al. (2016) and Hassanin et al. (2016) for *Cytb* sequences of additional species, including *E. labiatus*, *E. crypturus*, *E. minimus*, and *E. minor*. By contrast, *Cytb* sequences of *E. wahlbergi* and *E. dobsonii* were found to be more divergent. The existence of two divergent haplogroups in the *Epomophorus* species complex is also confirmed by our mitogenomic analyses, and the first haplogroup can be further divided into three geographic groups corresponding to (a) the Horn of Africa, with *E. labiatus* from Djibouti; (b) the rainforest–savanna mosaics, with *E. gambianus* from Senegal to Central African Republic and *M. pusillus* from Gabon and Katanga (southeastern Democratic Republic of the Congo); and (c) the Zambezian woodlands, with *E. crypturus* from Katanga and South Africa, *E. minimus* from Katanga, *E. minor* from Tanzania, and *E. labiatus* from Malawi.

Our analyses of mitochondrial genomes also support the non-monophyly of four species, that is, *E. crypturus*, *E. gambianus*, *E. labiatus*, and *M. pusillus*. Although these patterns may be explained by taxonomic issues, such as species misidentification or synonymy, mitochondrial introgression between closely related species is an alternative hypothesis (e.g., Centeno-Cuadros et al., 2019; Hassanin et al., 2018). Indeed, such introgression has been advanced by Nesi et al. (2011) to explain why *E. gambianus* and *M. pusillus* share similar mitochondrial sequences, but different nuclear sequences. Our mitogenomic phylogeny suggests that the species identified as *E. crypturus*, *E. minimus*, *E. minor*, and *E. labiatus* might also be involved in woodlands of southern Africa with mitochondrial introgression. Nuclear data are, however, needed to fully assess this issue.

ACKNOWLEDGEMENTS

We thank our colleagues who helped us to collect tissue samples used in this study: Philippe Blot, André Délicat, Christiane Denys, Mireille Dosso, Jérôme Fuchs, Jean-Pierre Hugot, François Jacquet, Javier Juste, Julian Kerbis Peterhans, Kan Stéphane Kouassi, Alain Le Faou, Eric Leroy, Nicolas Nesi, Carine Ngoagouni, Anne Ropiquet, Manuel Ruedi, and Peter Vallo. We are very grateful to collection managers and curators who provided samples from museum specimens: Julia Betz, Katrin Krohmann, and Virginie Volpato (Naturmuseum Senckenberg, Frankfort, Germany); Christiane Funk, Lisa Kluckert, Nora Lange, and Frieder Mayer (Museum für Naturkunde, Berlin, Germany); Lawrence R. Heaney, John Phelps, and the late William Stanley (Field Museum, Chicago, USA); and Anne-Marie Ohler and Jean-Marc Pons (Muséum national d'Histoire naturelle, Paris, France). This work was supported by the LabEx BCDiv 2012–2013.

ORCID

Alexandre Hassanin https://orcid.org/0000-0002-4905-8540
Didier Tshikung https://orcid.org/0000-0002-1883-309X
Blaise Kadjo https://orcid.org/0000-0002-8147-6064
Emmanuel Nakouné https://orcid.org/0000-0002-4620-5824
Vuong Tan Tu https://orcid.org/0000-0002-5915-865X
Vincent Prié https://orcid.org/0000-0002-6261-3270
Steven M. Goodman https://orcid.org/0000-0001-9318-0570

REFERENCES

ACR (2018). *African Chiroptera report 2018* (pp. 1–802, i–xvi). Pretoria, South Africa: AfricanBats NPC. https://doi.org/10.13140/RG.2.2.18794.82881

Almeida, F. C., Giannini, N. P., DeSalle, R., & Simmons, N. B. (2011). Evolutionary relationships of the Old World fruit bats (Chiroptera, Pteropodidae): Another star phylogeny? *BMC Evolutionary Biology*, *11*, 281. https://doi.org/10.1186/1471-2148-11-281

Almeida, F. C., Giannini, N. P., & Simmons, N. B. (2016). The evolutionary history of the African fruit bats (Chiroptera: Pteropodidae). *Acta Chiropterologica*, *18*, 73–90. https://doi.org/10.3161/15081109ACC2016.18.1.003

Amador, L. I., Moyers Arévalo, R. L., Almeida, F. C., Catalano, S. A., & Giannini, N. P. (2018). Bat systematics in the light of unconstrained analyses of a comprehensive molecular supermatrix. *Journal of Mammalian Evolution*, *25*, 37–70. https://doi.org/10.1007/s10914-016-9363-8

Andersen, K. (1912). *Catalogue of the Chiroptera in the British Museum. Second Edition. Volume I: Megachiroptera* (pp. 1–854, i–ci). London, UK: Trustees of the British Museum (Natural History). https://doi.org/10.5962/bhl.title.8322

Arabi, J., Cruaud, C., Couloux, A., & Hassanin, A. (2010). Studying sources of incongruence in arthropod molecular phylogenies: Sea spiders (Pycnogonida) as a case study. *Comptes Rendus Biologies*, *333*, 438–453. https://doi.org/10.1016/j.crvi.2010.01.018

Bergmans, W. (1989). Taxonomy and biogeography of African fruit bats (Mammalia, Megachiroptera). 2. The genera *Micropteropus* Matschie, 1899, *Epomops* Gray, 1870, *Hypsignathus* H. Allen, 1861, *Nanonycteris* Matschie, 1899, and *Plerotes* Andersen, 1910. *Beaufortia*, *39*, 89–153.

Biltekin, D., Popescu, S.-M., Suc, J.-P., Quézel, P., Jiménez-Moreno, G., Yavuz, N., & Çağatay, M. N. (2015). Anatolia: A long-time plant refuge area documented by pollen records over the last 23 million years. *Review of Palaeobotany and Palynology*, *215*, 1–22. https://doi.org/10.1016/j.revpalbo.2014.12.004

Boonman, A., Bumrungsri, S., & Yovel, Y. (2014). Nonecholocating fruit bats produce biosonar clicks with their wings. *Current Biology*, *24*, 2962–2967. https://doi.org/10.1016/j.cub.2014.10.077

Bouckaert, R., Heled, J., Kühnert, D., Vaughan, T., Wu, C.-H., Xie, D., … Drummond, A. J. (2014). BEAST2: A software platform for Bayesian evolutionary analysis. *PLoS Computational Biology*, *10*, e1003537. https://doi.org/10.1371/journal.pcbi.1003537.s001

Centeno-Cuadros, A., Razgour, O., García-Mudarra, J. L., Mingo-Casas, P., Sandonís, V., Redondo, A., … Juste, J. (2019). Comparative phylogeography and asymmetric hybridization between cryptic bat species. *Journal of Zoological Systematics and Evolutionary Research*, *57*, 1004–1018. https://doi.org/10.1111/jzs.12318

Ducrocq, S., Jaeger, J.-J., & Sige, B. (1993). Late Eocene southern Asian record of a megabat and its inferences on the megabat phylogeny. *Bat Research News*, *33*, 41–42.

Giannini, N. P., & Simmons, N. B. (2003). A phylogeny of megachiropteran bats (Mammalia: Chiroptera: Pteropodidae) based on direct optimization analysis of one nuclear and four mitochondrial genes. *Cladistics*, *19*, 496–511.

Gray, J. E. (1821). On the natural arrangement of vertebrose animals. *London Medical Repositories*, *15*, 296–310.

Gunnell, G. F., & Simmons, N. B. (2005). Fossil evidence and the origin of bats. *Journal of Mammalian Evolution*, *12*, 210–246. https://doi.org/10.1007/s10914-005-6945-2

Hamon, N., Sepulchre, P., Lefebvre, V., & Ramstein, G. (2013). The role of eastern Tethys seaway closure in the Middle Miocene Climatic Transition (ca. 14 Ma). *Climate of the Past*, *9*, 2687–2702. https://doi.org/10.5194/cp-9-2687-2013

Happold, M., & Happold, D. (2013). *Mammals of Africa. Volume IV: Hedgehogs, shrews and bats*. London, UK: Bloomsbury Publishing.

Hassanin, A. (2014). Description of a new bat species of the tribe Scotonycterini (Chiroptera, Pteropodidae) from southwestern Cameroon. *Comptes Rendus Biologies*, *337*, 134–142. https://doi.org/10.1016/j.crvi.2013.12.006

Hassanin, A., Bonillo, C., Nguyen, B. X., & Cruaud, C. (2010). Comparisons between mitochondrial genomes of domestic goat (*Capra hircus*) reveal the presence of numts and multiple sequencing errors. *Mitochondrial DNA*, *21*, 68–76. https://doi.org/10.3109/19401736.2010.490583

Hassanin, A., Colombo, R., Gembu, G. C., Merle, M., Tu, V. T., Görföl, T., … Ing, R. K. (2018). Multilocus phylogeny and species delimitation within the genus *Glauconycteris* (Chiroptera, Vespertilionidae), with the description of a new bat species from the Tshopo Province of the Democratic Republic of the Congo. *Journal of Zoological Systematics and Evolutionary Research*, *56*, 1–22. https://doi.org/10.1111/jzs.12176

Hassanin, A., Delsuc, F., Ropiquet, A., Hammer, C., Jansen van Vuuren, B., Matthee, C., … Couloux, A. (2012). Pattern and timing of diversification of Cetartiodactyla (Mammalia, Laurasiatheria), as revealed by a comprehensive analysis of mitochondrial genomes. *Comptes Rendus Biologies*, *335*, 32–50. https://doi.org/10.1016/j.crvi.2011.11.002

Hassanin, A., Khouider, S., Gembu, G.-C., Goodman, S. M., Kadjo, B., Nesi, N., … Bonillo, C. (2015). The comparative phylogeography of fruit bats of the tribe Scotonycterini (Chiroptera, Pteropodidae) reveals cryptic species diversity related to African Pleistocene forest refugia. *Comptes Rendus Biologies*, *338*, 197–211. https://doi.org/10.1016/j.crvi.2014.12.003

Hassanin, A., Léger, N., & Deutsch, J. (2005). Evidence for multiple reversals of asymmetric mutational constraints during the evolution of the mitochondrial genome of Metazoa, and consequences for phylogenetic inferences. *Systematic Biology*, *54*, 277–298.

Hassanin, A., Nesi, N., Marin, J., Kadjo, B., Pourrut, X., Leroy, E., … Bonillo, C. (2016). Comparative phylogeography of African fruit bats (Chiroptera, Pteropodidae) provides new insights into the outbreak of Ebola virus disease in West Africa, 2014–2016. *Comptes Rendus Biologies*, *339*, 517–528. https://doi.org/10.1016/j.crvi.2016.09.005

Hassanin, A., Ropiquet, A., Couloux, A., & Cruaud, C. (2009). Evolution of the mitochondrial genome in mammals living at high altitude: New insights from a study of the tribe Caprini (Bovidae, Antilopinae). *Journal of Molecular Evolution*, *68*, 293–310. https://doi.org/10.1007/s00239-009-9208-7

Hinsinger, D. D., Debruyne, R., Thomas, M., Denys, G. P. J., Mennesson, M., Utge, J., & Dettai, A. (2015). Fishing for barcodes in the Torrent: From COI to complete mitogenomes on NGS platforms. *DNA Barcodes*, *3*, 170–186. https://doi.org/10.1515/dna-2015-0019

Hoelzel, A. R., Lopez, J. V., Dover, G. A., & O'Brien, S. J. (1994). Rapid evolution of a heteroplasmic repetitive sequence in the mitochondrial DNA control region of Carnivores. *Journal of Molecular Evolution*, *39*, 191–199.

IUCN (2019). *The IUCN Red List of Threatened Species. Version 2019-1*. Retrieved from http://www.iucnredlist.org. Downloaded on 6 March 2019.

Juste, B. J., Alvarez, Y., Tabarés, E., Garrido-Pertierra, A., Ibáñez, C., & Bautista, J. M. (1999). Phylogeography of African fruitbats (Megachiroptera). *Molecular Phylogenetics and Evolution*, *13*, 596–604.

Kingdon, J. (1974). *East African mammals: An atlas of evolution in Africa. Volume 2, Part A. (Insectivores and Bats)*. London, UK: Academic Press.

Kunz, T. H. (1982). Roosting ecology of bats. In T. H. Kunz (Ed.), *Ecology of bats* (pp. 1–55). Boston, MA: Springer. https://doi.org/10.1007/978-1-4613-3421-7_1.

Kürschner, H. (1998). Biogeography and introduction to vegetation. In S. A. Ghazanfar & M. Fisher (Eds.), *Vegetation of the Arabian Peninsula* (pp. 63–98). Dordrecht, the Netherlands: Kluwer Academic Publishers.

Larsson, A. (2014). AliView: A fast and lightweight alignment viewer and editor for large data sets. *Bioinformatics*, *30*, 3276–3278. https://doi.org/10.1093/bioinformatics/btu531

Lê, S., Josse, J., & Husson, F. (2008). FactoMineR: An R package for multivariate analysis. *Journal of Statistical Software*, *25*, 1–18.

Lobry, J. R. (1995). Properties of a general model of DNA evolution under no-strand-bias conditions. *Journal of Molecular Evolution*, *40*, 326–330.

Meredith, R. W., Janečka, J. E., Gatesy, J., Ryder, O. A., Fisher, C. A., Teeling, E. C., … Murphy, W. J. (2011). Impacts of the Cretaceous terrestrial revolution and KPg extinction on mammal diversification. *Science*, *334*, 521–524. https://doi.org/10.1126/science.1211028

Meulenkamp, J. E., & Sissingh, W. (2003). Tertiary palaeogeography and tectonostratigraphic evolution of the Northern and Southern Peri-Tethys platforms and the intermediate domains of the African-Eurasian convergent plate boundary zone. *Palaeogeography, Palaeoclimatology, Palaeoecology*, *196*, 209–228.

Miller, M. A., Pfeiffer, W., & Schwartz, T. (2010). Creating the CIPRES Science Gateway for inference of large phylogenetic trees. In *Proceedings of the Gateway Computing Environments Workshop (GCE)*, 14 Nov. 2010, New Orleans, LA, pp. 1–8.

Nesi, N., Kadjo, B., Pourrut, X., Leroy, E., Pongombo Shongo, C., Cruaud, C., & Hassanin, A. (2013). Molecular systematics and phylogeography of the tribe Myonycterini (Mammalia, Pteropodidae) inferred from mitochondrial and nuclear markers. *Molecular Phylogenetics and Evolution*, *66*, 126–137. https://doi.org/10.1016/j.ympev.2012.09.028

Nesi, N., Nakouné, E., Cruaud, C., & Hassanin, A. (2011). DNA barcoding of African fruit bats (Mammalia, Pteropodidae). The mitochondrial genome does not provide a reliable discrimination between *Epomophorus gambianus* and *Micropteropus pusillus*. *Comptes Rendus Biologies*, *334*, 544–554. https://doi.org/10.1016/j.crvi.2011.05.003

Patnaik, R. (2016). Neogene-quaternary mammalian paleobiogeography of the Indian subcontinent: An appraisal. *Comptes Rendus Palevol*, *15*, 889–902. https://doi.org/10.1016/j.crpv.2015.11.004

Pound, M. J., Haywood, A. M., Salzmann, U., Riding, J. B., Lunt, D. J., & Hunter, S. J. (2011). A Tortonian (Late Miocene, 11.61-7.25 Ma) global vegetation reconstruction. *Palaeogeography, Palaeoclimatology, Palaeoecology*, *300*, 29–45.

Raghuram, H., Gopukumar, N., & Sripathi, K. (2007). Presence of single as well as double clicks in the echolocation signals of a fruit bat, *Rousettus leschenaulti* (Chiroptera: Pteropodidae). *Folia Zoologica*, *56*, 33–38.

Reyes, A., Gissi, C., Pesole, G., & Saccone, C. (1998). Asymmetrical directional mutation pressure in the mitochondrial genome of mammals. *Molecular Biology and Evolution*, *15*, 957–966.

Richter, H. V., & Cumming, G. S. (2008). First application of satellite telemetry to track African straw-coloured fruit bat migration. *Journal of Zoology*, *275*, 172–176. https://doi.org/10.1111/j.1469-7998.2008.00425.x

Roberts, L. H. (1975). Confirmation of the echolocation pulse production mechanism of *Rousettus*. *Journal of Mammalogy*, *56*, 218–220.

Ronquist, F., Teslenko, M., van der Mark, P., Ayres, D. L., Darling, A., Höhna, S., … Huelsenbeck, J. P. (2012). MrBayes 3.2: Efficient Bayesian phylogenetic inference and model choice across a large model space. *Systematic Biology*, *61*, 539–542. https://doi.org/10.1093/sysbio/sys029

Ropiquet, A., Li, B., & Hassanin, A. (2009). SuperTRI: A new approach based on branch support analyses of multiple independent data sets for assessing reliability of phylogenetic inferences. *Comptes Rendus Biologies*, *332*, 832–847. https://doi.org/10.1016/j.crvi.2009.05.001

Schoeman, M. C., & Goodman, S. M. (2012). Vocalizations in the Malagasy cave-dwelling fruit bat, *Eidolon dupreanum*: Possible evidence of incipient echolocation? *Acta Chiropterologica*, *14*, 409–416. https://doi.org/10.3161/150811012X661729

Senut, B., Pickford, M., & Ségalen, L. (2009). Neogene desertification of Africa. *Comptes Rendus Geoscience*, *341*, 591–602. https://doi.org/10.1016/j.crte.2009.03.008

Shi, J. J., Chan, L. M., Peel, A. J., Lai, R., Yoder, A. D., & Goodman, S. M. (2014). A deep divergence time between sister species of Eidolon (Pteropodidae) with evidence for widespread panmixia. *Acta Chiropterologica*, *16*, 279–292. https://doi.org/10.3161/150811014X687242

Shi, J. J., & Rabosky, D. L. (2015). Speciation dynamics during the global radiation of extant bats. *Evolution*, *69*, 1528–1545. https://doi.org/10.1111/evo.12681

Stamatakis, A. (2014). RAxML version 8: A tool for phylogenetic analysis and post-analysis of large phylogenies. *Bioinformatics*, *30*, 1312–1313. https://doi.org/10.1093/bioinformatics/btu033

Swofford, D. L. (2003). *PAUP*. Phylogenetic analysis using parsimony (*and other methods). Version 4*. Sunderland, MA: Sinauer Associates.

Teeling, E. C., Springer, M. S., Madsen, O., Bates, P., O'Brien, S. J., & Murphy, W. J. (2005). A molecular phylogeny for bats illuminates biogeography and the fossil record. *Science*, *307*, 580–584.

Utescher, T., Mosbrugger, V., Ivanov, D., & Dilcher, D. L. (2009). Present-day climatic equivalents of European Cenozoic climates. *Earth and Planetary Science Letters*, *284*, 544–552.

Yovel, Y., Geva-Sagiv, M., & Ulanovsky, N. (2011). Click-based echolocation in bats: Not so primitive after all. *Journal of Comparative Physiology. A, Neuroethology, Sensory, Neural, and Behavioral Physiology*, *197*, 515–530. https://doi.org/10.1007/s00359-011-0639-4

Zachos, J. C., Dickens, G. R., & Zeebe, R. E. (2008). An early Cenozoic perspective on greenhouse warming and carbon-cycle dynamics. *Nature*, *451*, 279–283. https://doi.org/10.1038/nature06588

Zachos, J., Pagani, M., Sloan, L., Thomas, E., & Billups, K. (2001). Trends, rhythms, and aberrations in global climate 65 Ma to present. *Science*, *292*, 686–693.

Zhang, Y. G., Pagani, M., Liu, Z., Bohaty, S. M., & Deconto, R. (2013). A 40-million-year history of atmospheric CO_2. *Philosophical Transactions. Series A, Mathematical, Physical, and Engineering Sciences*, *371*. 20130096.https://doi.org/10.1098/rsta.2013.0096

SUPPORTING INFORMATION

Additional supporting information may be found online in the Supporting Information section at the end of the article.

Table S1. Primers used for PCR amplification and Sanger DNA sequencing.

Table S2. Base composition of the 126 mtDNA genomes.

Table S3. Bayesian node ages (95% HPD in million years ago) estimated using either the mtDNA or mtDNA-Tv datasets and two different third calibration points (P1: MRCA of Pteropus + Nyctimene = 16.4 1.1 Mya; P2: MRCA of Pteropodidae = 25.0 2.0 Mya).

Figure S1. RAxML trees inferred from the four datasets (*mtDNA*, *mtDNA-Tv*, *PCG-DNA*, *PCG-AA*).

Figure S2. Bayesian tree reconstructed from the *mtDNA* alignment (126 taxa and 15,448 nt).

How to cite this article: Hassanin A, Bonillo C, Tshikung D, et al. Phylogeny of African fruit bats (Chiroptera, Pteropodidae) based on complete mitochondrial genomes. *J Zool Syst Evol Res*. 2020;58:1395–1410. https://doi.org/10.1111/jzs.12373

APPENDIX 1

Taxa and specimens sequenced in the present study

Tribe	Subtribe	Species	Sample code	Voucher specimen	Country of origin	Sequencing method	Length (bp)	GenBank accession No.
Eonycterini	NA	*Eonycteris spelaea*	JPH05	NA	Thailand	Sanger	16,700	MN816308
Eonycterini	NA	*Eonycteris spelaea*	VN410	NA	Vietnam	Sanger + Ion	16,514	MN816309
Epomophorini	Epomophorina	*Epomophorus crypturus*	T310	NA	South Africa	Sanger	16,825	MN816311
Epomophorini	Epomophorina	*Epomophorus crypturus*	K09378	MNHN ZM2011-772	DRC	Sanger	16,733	MN816310
Epomophorini	Epomophorina	*Epomophorus dobsonii*	T674	SMF 91296	Malawi	Sanger + Ion	16,543	MN816324
Epomophorini	Epomophorina	*Epomophorus gambianus*	3320	NA	Senegal	Sanger	16,799	MN816312
Epomophorini	Epomophorina	*Epomophorus gambianus*	R085	MNHN ZM2011-685	CAR	Sanger	16,798	MN816313
Epomophorini	Epomophorina	*Epomophorus labiatus*	T273	MNHN ZM2000-553	Djibouti	Sanger	16,741	MN816315
Epomophorini	Epomophorina	*Epomophorus labiatus*	T689	SMF 93228	Malawi	Sanger	16,636	MN816316
Epomophorini	Epomophorina	*Epomophorus minimus*	K09222	MNHN ZM2011-792	DRC	Sanger	16,743	MN816318
Epomophorini	Epomophorina	*Epomophorus minor*	T667	FMNH 171299	Tanzania	Sanger	16,849	MN816319
Epomophorini	Epomophorina	*Epomophorus* sp1	K09224	MNHN ZM2011-726	DRC	Sanger + Ion	16,693	MN816314
Epomophorini	Epomophorina	*Epomophorus* sp2	K09227	MNHN ZM2011-760	DRC	Sanger	16,734	MN816320
Epomophorini	Epomophorina	*Epomophorus wahlbergi*	K0935	MNHN ZM2011-787	DRC	Sanger	16,668	MN816317
Epomophorini	Epomophorina	*Epomophorus wahlbergi*	K09325	MNHN ZM2011-800	DRC	Sanger	16,725	MN816321
Epomophorini	Epomophorina	*Epomophorus wahlbergi*	T666	FMNH 187408	Tanzania	Sanger	16,662	MN816322
Epomophorini	Epomophorina	*Epomops buettikoferi*	G093	NA	RCI	Sanger	16,867	MN816323
Epomophorini	Epomophorina	*Epomops franqueti*	1427	NA	Gabon	Sanger + Ion	16,686	MN816325
Epomophorini	Epomophorina	*Hypsignathus monstrosus*	1699	NA	Gabon	Sanger	16,738	MN816326
Epomophorini	Epomophorina	*Micropteropus pusillus*	1566	NA	Gabon	Sanger	16,727	MN816332
Epomophorini	Epomophorina	*Micropteropus pusillus*	K0970	MNHN ZM2011-840	DRC	Sanger	16,728	MN816333
Epomophorini	Epomophorina	*Nanonycteris veldkampii*	T180	NA	CAR	Sanger	16,699	MN816340
Epomophorini	Epomophorina	*Nanonycteris veldkampii*	G0939	NA	RCI	Sanger	16,699	MN816341
Epomophorini	Myonycterina	*Megaloglossus azagnyi*	G0970	NA	RCI	Sanger + Ion	16,538	MN816329
Epomophorini	Myonycterina	*Megaloglossus woermanni*	1538	NA	Gabon	Sanger	16,632	MN816330
Epomophorini	Myonycterina	*Megaloglossus woermanni*	T702	SMF 84408	DRC	Sanger	16,715	MN816331
Epomophorini	Myonycterina	*Myonycteris angolensis*	G0935	NA	RCI	Sanger + Ion	16,566	MN816334
Epomophorini	Myonycterina	*Myonycteris angolensis*	K09300	MNHN ZM2011-806	DRC	Sanger + Ion	16,544	MN816335
Epomophorini	Myonycterina	*Myonycteris brachycephala*	T672	ST 105	Sao Tomé	Sanger + Ion	16,814	MN816336
Epomophorini	Myonycterina	*Myonycteris leptodon*	G0944	NA	RCI	Sanger + Ion	16,493	MN816337
Epomophorini	Myonycterina	*Myonycteris relicta*	T668	FMNH 151404	Tanzania	Sanger + Ion	16,715	MN816338

TABLE 1 (Continued)

Tribe	Subtribe	Species	Sample code	Voucher specimen	Country of origin	Sequencing method	Length (bp)	GenBank accession No.
Epomophorini	Myonycterina	*Myonycteris torquata*	1732	NA	Gabon	Sanger + Ion	16,728	MN816339
Epomophorini	Plerotina	*Plerotes anchietae*	K09279	MNHN ZM2011-860	DRC	Sanger	16,799	MN816343
Epomophorini	Stenonycterina	*Stenonycteris lanosus*	T670	FMNH 151178	Tanzania	Sanger	16,801	MN816365
Rousettini	NA	*Rousettus aegyptiacus*	1412	NA	Gabon	Sanger	16,674	MN816345
Rousettini	NA	*Rousettus aegyptiacus*	K09235	MNHN ZM2011-862	DRC	Sanger	16,732	MN816346
Rousettini	NA	*Rousettus aegyptiacus*	K09236	MNHN ZM2011-863	DRC	Sanger	16,659	MN816347
Rousettini	NA	*Rousettus aegyptiacus*	T246	NA	Senegal	Sanger	16,733	MN816348
Rousettini	NA	*Rousettus aegyptiacus*	T2206	MHNG 1807.092	Cyprus	Sanger	16,753	MN816349
Rousettini	NA	*Rousettus aegyptiacus*	T2209	NA	Egypt	Sanger + Ion	16,742	MN816350
Rousettini	NA	*Rousettus aegyptiacus*	T2219	MHNG 1971.070	Malawi	Sanger + Ion	16,671	MN816351
Rousettini	NA	*Rousettus amplexicaudatus*	CKM76	NA	Cambodia	Sanger	16,573	MN816352
Rousettini	NA	*Rousettus amplexicaudatus*	VN1368	NA	Vietnam	Sanger + Ion	16,720	MN816353
Rousettini	NA	*Rousettus leschenaulti*	CKM109	NA	Cambodia	Sanger	16,655	MN816354
Rousettini	NA	*Rousettus leschenaulti*	VN431	NA	Vietnam	Sanger	16,703	MN816355
Rousettini	NA	*Rousettus madagascariensis*	T2204	UADBA 43761	Madagascar	Sanger	16,777	MN816356
Rousettini	NA	*Rousettus madagascariensis*	T2205	UADBA 43762	Madagascar	Sanger	16,787	MN816357
Rousettini	NA	*Rousettus obliviousus*	T2199	FMNH 220017	Madagascar	Sanger	16,636	MN816358
Rousettini	NA	*Rousettus obliviousus*	T2202	FMNH 220042	Madagascar	Sanger	16,708	MN816359
Scotonycterini	NA	*Casinycteris argynnis*	2209	NA	Gabon	Sanger	16,661	MN816299
Scotonycterini	NA	*Casinycteris argynnis*	R08126	MNHN ZM2011-683	CAR	Sanger + Ion	16,637	MN816300
Scotonycterini	NA	*Casinycteris campomaanensis*	C0741	MNHN ZM2011-637	Cameroon	Sanger	16,630	MN816301
Scotonycterini	NA	*Casinycteris ophiodon*	T690	SMF 91850	RCI	Sanger	16,631	MN816302
Scotonycterini	NA	*Casinycteris ophiodon*	ZMB5001	ZMB5001	Cameroon	Illumina	16,477	MN816303
Scotonycterini	NA	*Scotonycteris bergmansi*	1337	NA	Gabon	Sanger	16,727	MN816360
Scotonycterini	NA	*Scotonycteris bergmansi*	F149402	FMNH 149402	DRC	Sanger	16,711	MN816361
Scotonycterini	NA	*Scotonycteris occidentalis*	G09106	NA	RCI	Sanger + Ion	16,666	MN816362
Scotonycterini	NA	*Scotonycteris zenkeri*	C0740	MNHN ZM2011-682	Cameroon	Sanger	16,731	MN816363

(Continues)

TABLE 1 (Continued)

Tribe	Subtribe	Species	Sample code	Voucher specimen	Country of origin	Sequencing method	Length (bp)	GenBank accession No.
Outgroup	NA	*Cynopterus brachyotis*	140810x2	NA	NA	Sanger + Ion	16,750	MN816304
Outgroup	NA	*Cynopterus sphinx*	CKM35	NA	Cambodia	Sanger + Ion	16,897	MN816305
Outgroup	NA	*Dobsonia* sp.	050810x2F	NA	NA	Sanger + Ion	16,808	MN816306
Outgroup	NA	*Eidolon helvum*	1535	NA	Gabon	Sanger	16,764	MN816307
Outgroup	NA	*Macroglossus sobrinus*	JPH07	NA	Thailand	Sanger	16,415	MN816327
Outgroup	NA	*Megaerops niphanae*	NLN25	NA	Lao PDR	Sanger + Ion	16,604	MN816328
Outgroup	NA	*Nyctimene cephalotes*	180810x3	NA	NA	Sanger + Ion	16,702	MN816342
Outgroup	NA	*Pteropus tonganus*	T275	NA	NA	Sanger	16,718	MN816344
Outgroup	NA	*Sphaerias blanfordi*	LNK94	NA	Lao PDR	Sanger	16,776	MN816364

Abbreviations: Ion, Ion Torrent; NA, not applicable.